Scattering of sine-Gordon kinks on potential wells

2007 J. Phys. A: Math. Theor. 40 5995

(http://iopscience.iop.org/1751-8121/40/22/016)

IOP PUBLISHING JOURNAL OF PHYSICS A: MATHEMATICAL AND THEORETICAL

J. Phys. A: Math. Theor. **40** (2007) 5995–6010 doi:10.1088/1751-8113/40/22/016

Scattering of sine-Gordon kinks on potential wells

Bernard Piette and W J Zakrzewski

Department of Mathematical Sciences, University of Durham, Science Laboratories, South Road, Durham DH1 3LE, UK

Received 6 November 2006, in final form 16 April 2007
Published 14 May 2007
Online at stacks.iop.org/JPhysA/40/5995

Abstract

We study the scattering properties of sine-Gordon kinks on obstructions in the form of finite size potential 'wells'. We model this by making the coefficient of the $\cos(\varphi) - 1$ term in the Lagrangian position dependent. We show that when the kinks find themselves in the well they radiate and then interact with this radiation. As a result of this energy loss, the kinks become trapped for small velocities while at higher velocities they are transmitted with a loss of energy. However, the interaction with the radiation can produce 'unexpected' reflections by the well. We present two simple models which capture the gross features of this behaviour. Both involve standing waves either at the edges of the well or in the well itself.

PACS numbers: 11.10.Lm, 12.39.Dc, 03.75.Lm

1. Introduction

Recently [1], we have performed a detailed study of scattering properties of (2+1)-dimensional topological solitons on potential wells. This work was based on the 'baby' Skyrme model, i.e. we used the Lagrangian density which consisted of three terms: the pure $\mathcal{S}^2$ sigma model, the Skyrme and the potential terms:

$$\mathcal{L} = \partial_\mu \vec{\phi} \cdot \partial^\mu \vec{\phi} - \theta_S[(\partial_\mu \vec{\phi} \cdot \partial^\mu \vec{\phi})^2 - (\partial_\mu \vec{\phi} \cdot \partial_\nu \vec{\phi})(\partial^\mu \vec{\phi} \cdot \partial^\nu \vec{\phi})] - V(\vec{\phi}) \tag{1}$$

where

$$V(\phi) = \mu\big(1 - \phi_3^2\big). \tag{2}$$

The vector $\vec{\phi}$ was restricted to lie on a unit sphere $\mathcal{S}^2$ hence we put $\vec{\phi} \cdot \vec{\phi} = 1$.

To generate the potential well, the coefficient of the potential term μ was made x dependent. For x outside the well it had one value, say, μ_{out} and inside the well, i.e. for $a < x < b$, its value was reduced to μ_{in}. This choice of μ did not affect the vacuum (taken as $\phi_3 = +1$); the skyrmion was given by a field configuration which varied from $\phi_3 = +1$ far away from the position of the skyrmion to $\phi_3 = -1$ at its position. Initially, the skyrmions were placed far

away from the 'well' (so that all the variation of ϕ_3 from +1 took place for x well away from the 'well', i.e. for $x < a$).

The 'skyrmions' were then sent towards the well and their properties were studied. The obtained results have shown that when the solitons fall into the 'well' they get deformed and this deformation may excite the vibrational modes of the skyrmion and may lead to the skyrmions radiating away their excess of energy. In consequence, the skyrmions can get 'trapped' in the well or emerge from it with a reduced velocity. In [2] we presented a simple four mass model which apes the vibrational modes of the skyrmion and we showed that many of the observed scattering properties of skyrmions can be reproduced in this model—suggesting that their origin resides in the excitation of the lowest vibrational modes of the skyrmion.

Given this, it is important to check what happens in models in which the solitons have fewer vibrational modes and so we have decided to look at the (1+1)-dimensional sine-Gordon model and see what happens when its kinks scatter on the potential wells.

In the next section, we discuss our results obtained for the sine-Gordon model. In this model we include a finite size, finite depth, potential well which is introduced by appropriately modifying the coefficient of the nonlinear term in the Lagrangian. The results are qualitatively similar to what we have seen in the two-dimensional model and are not very different from the results obtained some time ago by Fei *et al* [3], in a work which involved the scattering of sine-Gordon kinks on a one-point impurity.

The idea of studying the scattering of sine-Gordon kinks on defects has a long history. Campbell and Peyrard [4, 5] have generalized the earlier work on kink–antikink interactions in $\lambda\phi^4$ theory [6] to the sine-Gordon model. Their work presented very elegant physical arguments that stressed the importance of the waves that get generated during the interaction. A general review of this work and of the other work on soliton dynamics in perturbed sine-Gordon equations can be found in [7]. The work of Campbell and Peyrard has inspired Goodman and collaborators to study the effects of defects further. Their early papers [8, 9] dealt mainly with studying the effects in optics and they have finally led to their 'two-bounce' resonance model [10]. In this 'two-bounce' model Goodman *et al* [10] have managed to explain the old results of Fei *et al* [3] in some detail. Their model, which in fact is based on the original idea of Fei *et al* [3] (see also a recent review [11]), associates the observed phenomena with the interaction between the kink and the waves that describe the oscillation of the vacuum (around the impurity) and which get generated by the passage of the kink. This interaction is described by very specific modes and only the strength of these modes can vary during the scattering process.

The sine-Gordon equation is used to describe a very wide range of physical systems including, amongst others, the Josephson effects [12], particle physics [13], information transport in microtubules [14], nonlinear optics [15] and ferromagnets [16]. After the introduction of dimensionless variables, one is usually left with the sine-Gordon equation with a coefficient λ multiplying the $\sin(\phi)$ term and such that this coefficient is related to the physical parameters of the system. In homogeneous media, λ is simply a constant parameter, but in an inhomogeneous medium λ becomes a function of x. For example, in microtubules, λ is proportional to the dipole density in the vicinal water in brain microtubules [14]. In nonlinear optics λ is proportional to the dipole moment density and inversely proportional to the dielectric constant of the medium [15]. In an inhomogeneous medium, λ would thus be very much like the potential that we consider in this paper. In ferromagnetic chains, λ is proportional to both the magnetic moment of the medium and the magnetic field in which the chain is immersed. Again, one could consider inhomogeneous media or experiments in which the magnetic field is position dependent.

In their work, Fei *et al* and Goodman have only considered the sine-Gordon model with a delta-like potential which describe media containing impurities. In this paper, we consider the more general case of a well of finite depth and finite width which correspond to genuine inhomogeneous media.

The model of Goodman *et al* has reproduced all the features of the results of the original simulations reported in [3]. Hence, in the following section we introduce a similar model for our case which now involves a finite well of width $2p$ and depth $1 - \lambda$. To do this we make an ansatz for an approximate field which describes the system. It involves a sine-Gordon kink which is allowed to alter its slope and we add to it two amplitudes of oscillation of the vacuum (at each end of the 'well').

In section 3, we derive the Lagrangian for such an effective model from the original Lagrangian. As the model is somewhat crude we make some drastic approximations in our derivation of the Lagrangian but still find that the model reproduces the main features of the scattering reasonably well. Hence, we believe the ideas of Goodman and collaborators to be correct and be more general in nature—thus showing that due to the interaction of the soliton with the radiation in the well its behaviour can be quite complicated and can result in the reflection of the soliton by the well, i.e. a process which is purely classical in nature but could be confused with a quantum behaviour. To confirm this further we introduce a further model (with a couple of radiation standing waves in the well) and again reproduce the main features of the full scattering process.

The last section presents some concluding remarks.

2. Sine-Gordon model and its kinks

We take the Lagrangian of the (1+1)-dimensional sine-Gordon model in the form

$$\mathcal{L} = \partial_\mu \varphi \cdot \partial^\mu \varphi - \lambda^2 \sin(\varphi)^2, \tag{3}$$

where, for the kink, the basic field φ goes from 0 at $x = -\infty$ to π at $= \infty$. In the static case its explicit form is

$$\varphi(x) = 2\tan^{-1}(\exp(\theta(x - x_0)), \tag{4}$$

where x_0 is the kink's position and θ is its slope. For (4) to be a solution of the equations of motion which follow from (3) we need to set $\theta = \lambda$.

To have a 'well' we set

$$\lambda = \begin{cases} 1 & \text{for} \quad |x| > p \\ \lambda_0 & \text{for} \quad |x| < p. \end{cases} \tag{5}$$

Clearly, $\lambda_0 < 1$ describes a well while $\lambda_0 > 1$ describes a barrier. As the two-dimensional studies gave more interesting results for the wells in this paper we restrict our attention to $\lambda_0 < 1$.

We have performed many numerical simulations, varying λ_0 and p (the width of the well).

2.1. Numerical simulations

We have performed most of our simulations using a 10001-point lattice with the lattice spacing being 0.05. Hence our lattice extended from −50 to +50. The kink was initially placed at $x_0 = -40$. Its size was determined by $\theta = 1$ which means that its field was essentially $\varphi \sim 0$ for $x < -45$ and $\varphi \sim \pi$ for $x > -35$. Thus, there were no problems with any boundary effects (we have verified this by altering the lattice size and x_0).

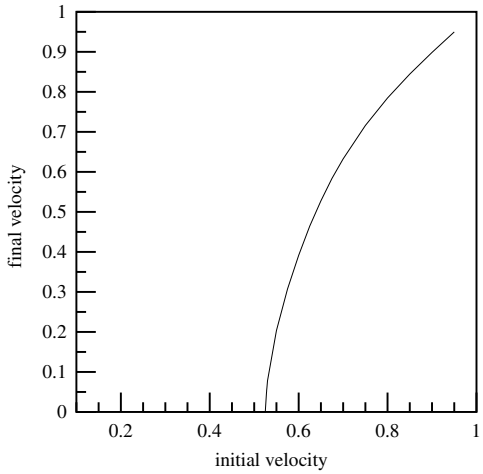

Figure 1. Velocity of the kink leaving the well as a function of its velocity as it approaches the well ($p = 5, \lambda_0 = 0.2$).

We have performed three sets of simulations: one involving a very narrow 'well' ($p = 0.5$) and two involving a larger well ($p = 5$) (one shallow—$\lambda_0 = 0.8$ and one rather deep—$\lambda_0 = 0.2$). In each case we sent the kink (originally at $x_0 = -40$) towards the well varying its initial velocity. To do this we took the expression for a kink moving with velocity v, i.e.,

$$\varphi(x,t) = 2\tan^{-1}(\exp(\gamma(x - x_0 - vt))), \qquad \gamma = \frac{1}{\sqrt{1-v^2}} \tag{6}$$

(obtained by Lorentz boosting (4) and setting $\theta = 1$) and then used it to calculate the initial conditions ($\varphi(x,0)$ and $\frac{\partial\varphi(x,0)}{\partial t}$).

All our simulations were performed using a fourth-order Runge–Kutta method for simulating the time evolution. The time step of our simulations was taken to be 0.0001. We used fixed boundary conditions and later we also used absorbing boundary conditions at the edges of the lattice. This was generated by successively decreasing the magnitude of $\frac{\partial\varphi}{\partial t}$ for the last 50 points at both ends of the lattice.

2.2. Deep well

In the deep well case we took $\lambda_0 = 0.2$ and $p = 5$. We have found that when the kink was in the well it radiated and so when it finally emerged from the well its velocity was lower than the initial velocity. This was due to the fact that the well distorted the soliton which then began vibrating (i.e. its slope started oscillating). These vibrations were then gradually converted into radiation with the slope settling at its original value. The curve of the final velocity as a function of the initial one is shown in figure 1. As is clear from the plot, the kink whose initial velocity is less than $v_{\rm cr} \sim 0.527$ gets trapped in the well. The curve is very smooth and, as expected, we note that for initial velocities larger than $v_{\rm cr}$ the final velocity is always smaller than the initial one demonstrating the loss of the kinetic energy of the kink through vibration resulting in radiation.

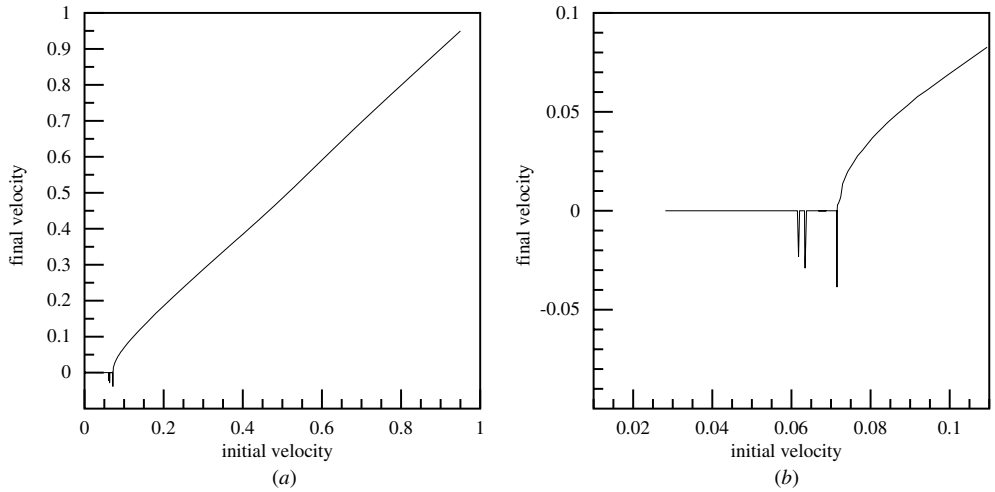

Figure 2. Velocity of the kink leaving the well as a function of its velocity as it approaches the well ($p = 5, \lambda_0 = 0.8$). (*a*) Full plot. (*b*) A close-up for small velocities.

2.3. Shallow well

For a shallow well we took $\lambda_0 = 0.8$ and still $p = 5$. This time the critical velocity is much smaller (as the well perturbs the kink much less). The curve of the outgoing velocity as a function of the incoming one is shown in figure 2(*a*).

Looking at the plot we note that there is some irregularity close to the threshold. Blowing it up (see figure 2(*b*)) we note that just below the critical velocity we also have some negative velocities (i.e. the whole process looks as if the kink was reflected by the well!). Thus in addition to trajectories like those in figures 3(*a*) and (*b*) we also have trajectories like those of figure 3(*c*)

Of course, the reflected trajectory is somewhat unexpected; this is what one would expect in a quantum system but here we have a completely classical system and we have a reflection by the well. Clearly, this reflection must be somewhat related to the interaction of the deformed kink with the radiation that is present in the well. To look at this in more detail we have also looked at a very narrow well.

2.4. Very narrow well

This time we took $p = 0.5$ and $\lambda_0 = 0.2$. The obtained curve of the velocities is shown in figure 4(*a*). Again we see an interesting behaviour close to the threshold, and blowing it up we get figure 4(*b*).

Are these results just numerical artefacts? To answer this question we have carried out several tests. First we changed the lattice size (increased the number of points, changed the lattice spacing) and changed the time step in the Runge–Kutta scheme. However, the observed pattern of reflections was reproduced in all simulations. We have also varied the discretization scheme and, among others, also considered the 'topological discretization' of Speight and Ward [17]. All simulations using these discretizations exhibited similar patterns, with the values of the outgoing velocities seen in all of them being essentially the same (the values differed only in the fourth decimal points). Of course, these velocities were always smaller

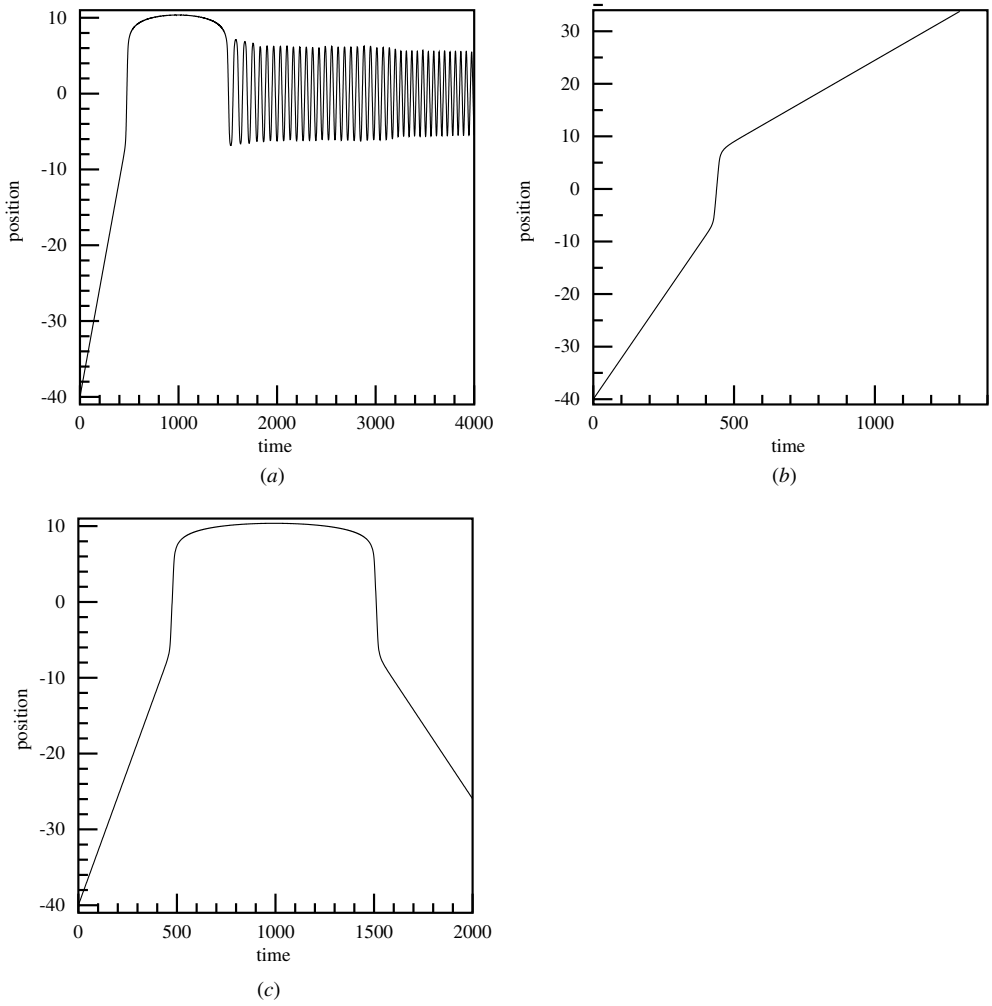

Figure 3. Typical trajectories ($p = 5, \lambda = 0.8$). (*a*) Below 'threshold' ($v = 0.071\,535$), (*b*) transmitted ($v = 0.077\,983$) and (*c*) reflected ($v = 0.071\,514$).

than the incoming ones. Hence, we believe the effect to be genuine and so we are left with having to explain its origin.

Performing a literature search we have found the above-mentioned paper by Fei *et al* [3]. In that paper the authors studied the scattering of sine-Gordon kinks on a one-lattice-point impurity (at one-lattice site the potential $\lambda\varphi^2$ was changed to a different value, $\lambda'\varphi^2$). Figure 11 of that paper looks amazingly similar to our figure 4(*b*). Of course, our potential corresponds to a superposition of defects of Fei *et al* so not surprisingly the pattern is more evident in a system involving a smaller well. However, the fact that the effect persists and is seen for larger wells suggests that the phenomenon is more fundamental in nature.

The phenomenon observed by Fei *et al* was recently explained by Goodwin *et al* [10] in terms of a two-mode model involving the interaction of the kink with the radiation at the impurity point. Clearly, in our case we have two special points (at the two 'edges' of the well where the potential changes). Hence, it may make sense to develop a model based on oscillations at these two points. This is what we do in the next section.

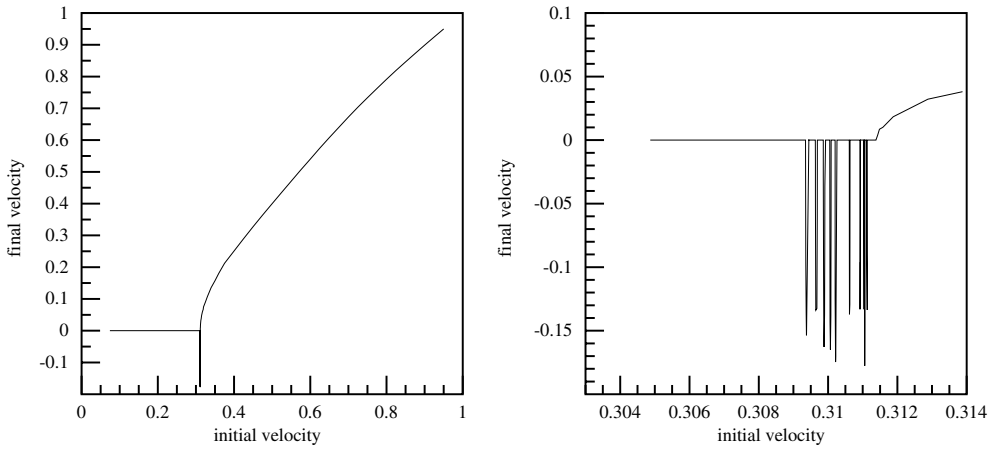

Figure 4. Velocity of the kink leaving the well as a function of its velocity as it approaches the well ($p = 0.5, \lambda_0 = 0.2$). (*a*) Full plot. (*b*) A close-up for small velocities.

3. Our effective model

Following Fei *et al* [3] and Goodman *et al* [10] we consider the following ansatz:

$$\varphi(x,t) = 2\tan^{-1}\exp(\theta(t)(x - x_0(t))) + a(t)g(x) + b(t)h(x), \tag{7}$$

where we take $g(x)$ and $h(x)$ in the form

$$g(x) = \exp\left(-\frac{|x-p|}{2}D\right), \qquad h(x) = \exp\left(-\frac{|x-p|}{2}F\right), \tag{8}$$

and

$$D = \begin{cases} A, & x > p \\ B, & x < p, \end{cases} \qquad F = \begin{cases} B, & x > -p \\ A, & x < -p. \end{cases} \tag{9}$$

Thus, we have allowed the kink to change its position $x_0(t)$ and its slope $\theta(t)$, and $a(t)$ and $b(t)$ represent the excitations of the vacuum. Our choice of functions $g(x)$ and $h(x)$ is motivated by the ideas of Goodman *et al* [10] who have shown that such a term describes well the response of the vacuum around the defect to an excitation. They have studied this in detail; the defect generates a standing wave which is well described by an exponential. In our case, we can think of the well as corresponding to two defects (its two edges) and so this motivates our choice of the ansatz (7)–(9). We thus ignore, for the time being, the standing waves inside the well. Of course, we do not expect it to be perfect; we only hope that it captures the main features of the phenomenon we are looking at.

To obtain an effective model we put this expression for $\varphi(x,t)$ into the Lagrangian density (3) and attempted to integrate it over x. However, as this leads to rather complicated expressions which we had not succeeded to calculate analytically we resorted to an expansion (in the perturbation due to the well). Hence we put $\varphi = \varphi_0 + \delta\varphi$, where

$$\varphi_0 = 2\tan^{-1}\exp(\theta(t)(x - x_0(t))) \tag{10}$$

and

$$\delta\varphi = a(t)g(x) + b(t)h(x). \tag{11}$$

Next, we expanded

$$\sin^2(\varphi_0+\delta\varphi) \sim \sin(\varphi_0)+\sin(2\varphi_0)\delta\varphi+\cos(2\varphi)(\delta\varphi)^2\cdots. \tag{12}$$

Then as

$$\frac{\partial\varphi}{\partial t}=2\cos^2\left(\frac{\varphi}{2}\right)[\dot\theta(x-x_0)-\theta\dot x_0]\,\mathrm{e}^{\theta(x-x_0)}+\dot a g(x)+\dot b h(x) \tag{13}$$

we found that

$$T_1=\int_{-\infty}^{\infty}\mathrm{d}x\left(\frac{\partial\varphi_0}{\partial t}\right)^2=\frac{1}{12}\frac{\pi^2\dot\theta^2}{\theta^3}+\theta\dot x_0^2. \tag{14}$$

The $\delta\varphi$ terms give us by themselves

$$T_2=\frac{1}{2}(\dot a^2+\dot b^2)\left(\frac{1}{B}+\frac{1}{A}\right)+\dot a\dot b\left[\frac{4}{A+B}\mathrm{e}^{-Bp}+\frac{2}{A-B}(\mathrm{e}^{-pB}-\mathrm{e}^{-pA})\right]. \tag{15}$$

Finally, we calculated the 'crossed terms' and we got (for the terms involving $\dot x_0$ and $\dot a$ and $\dot b$)

$$T_3=-2\theta\dot x_0\dot a\frac{K}{1+K^2}\left[\frac{1}{\theta+\frac{B}{2}}+\frac{1}{\frac{A}{2}-\theta}\right], \tag{16}$$

where $K=\exp(\theta(p-x_0))$ and a similar expression for $-2\theta\dot x_0\dot b$, except that this K was replaced by $\tilde K=\exp(\theta(-p-x_0))$. For the terms involving $\dot\theta$ and $\dot a$ we got

$$T_4=2\dot\theta\dot a\frac{K}{1+K^2}\left\{\left[\frac{1}{\left(\frac{A}{2}-\theta\right)^2}-\frac{1}{\left(\frac{B}{2}+\theta\right)^2}\right]+\frac{p(1-K^2)}{(1+K^2)}\left[\frac{1}{\theta+\frac{B}{2}}+\frac{1}{\frac{A}{2}-\theta}\right]\right\}. \tag{17}$$

The expression involving $\dot\theta\dot b$ was again the same with K replaced by $\tilde K$. These expressions are not exact; we obtained them by making several approximations of the type

$$K\int_0^{\infty}\mathrm{d}z\frac{\mathrm{e}^{-(\theta+\frac{B}{2})z}}{1+K^2\,\mathrm{e}^{-2\theta z}}\sim\frac{K}{1+K^2}\frac{1}{\left(\theta+\frac{B}{2}\right)}, \tag{18}$$

which should be reasonably reliable given the exponential form of the dependence of the integrands on z, etc.

Next, we calculated the contribution due to $\left(\frac{\partial\varphi}{\partial x}\right)^2$. Performing the integrations and making similar approximations as before we got

$$P_1=\theta+\frac{(a^2+b^2)}{8}+\frac{ab}{4}\left[4(A+B)\,\mathrm{e}^{-Bp}+\frac{(A+B)^2}{2(A-B)}(\mathrm{e}^{-pB}-\mathrm{e}^{-pA})\right] \tag{19}$$

plus terms linear in a and b. They are given by

$$P_2=-\frac{A+B}{2}\left(\frac{1}{\frac{A}{2}-\theta}+\frac{1}{\frac{B}{2}+\theta}\right)\left(\theta a\frac{K}{1+K^2}+\theta b\frac{\tilde K}{1+\tilde K^2}\right). \tag{20}$$

Finally, we had to add the terms coming from $\lambda^2\sin^2(\varphi)$. The contribution due to the well is given by

$$\begin{aligned}\lambda_0^2\int_{-p}^{p}\sin^2(\varphi_0)\,\mathrm{d}x&=\lambda_0^2\int_{-p}^{p}\frac{\mathrm{e}^{2\theta(x-x_0)}}{[1+\mathrm{e}^{2\theta(x-x_0)}]^2}\,\mathrm{d}x\\&=\frac{\lambda_0^2}{\theta}\frac{\sinh(2\theta p)}{\cosh(2\theta x_0)+\cosh(2\theta p)}.\end{aligned} \tag{21}$$

The contribution due to $\int_{-\infty}^{\infty}\mathrm{d}x\,\lambda_0^2\sin^2(\varphi)$ can be calculated in a similar way and we get

$$P_3=\frac{\lambda_1^2}{\theta} \tag{22}$$

from the φ_0 term,

$$P_4 = 2\lambda_1^2 \left(\frac{1}{\frac{A}{2} - \theta} + \frac{1}{\frac{B}{2} + \theta} \right) \left[a \frac{K(1-K^2)}{(1+K^2)^2} + b \frac{\tilde{K}(1-\tilde{K}^2)}{(1+\tilde{K}^2)^2} \right] \tag{23}$$

from the terms linear in $\delta\varphi$ and

$$P_5 = \frac{\lambda_1^2}{2} \left[(a^2+b^2) \left(\frac{1}{B} + \frac{1}{A} \right) + ab \left(\frac{4}{A+B} \mathrm{e}^{-Bp} + \frac{2}{A-B} (\mathrm{e}^{-pB} - \mathrm{e}^{-pA}) \right) \right]. \tag{24}$$

Adding all these terms together we get the Lagrangian for our effective model. This Lagrangian is given by

$$\begin{aligned} L = {} & \frac{\pi^2}{12} \frac{\dot{\theta}^2}{\theta^3} + \theta \dot{x}^2 + \frac{1}{2}(\dot{a}^2 + \dot{b}^2) B_0 + \dot{a}\dot{b} B_1 - 2\theta \dot{x}_0 (\dot{a} D_0(\theta) + \dot{b} D_1(\theta)) + 2\dot{\theta}(\dot{a} D_2(\theta) + \dot{b} D_3(\theta)) \\ & - \theta - \frac{(a^2+b^2)}{8}(A+B) - \frac{ab}{4} + \frac{A+B}{2} \theta (a D_0(\theta) + b D_1(\theta)) - 2\epsilon \lambda_1^2 D_6(\theta, x_0) \\ & - \frac{\lambda_1^2}{\theta} - 2\lambda_1^2 (a D_4(\theta) + b D_5(\theta)) - \lambda_1^2 \frac{ab}{2} B_1 - \lambda_1^2 \frac{(a^2+b^2)}{2} B_0, \end{aligned} \tag{25}$$

where

$$B_0 = \frac{1}{B} + \frac{1}{A}, \qquad B_1 = \frac{4}{A+B} \mathrm{e}^{-pB} + \frac{2}{A-B} (\mathrm{e}^{-pB} - \mathrm{e}^{-pA})$$

and where the seven functions D_i, $i = 0, \ldots, 6$, are given by

$$D_0(\theta) = \frac{K}{1+K^2} \left[\frac{1}{\theta + 0.5B} + \frac{1}{0.5A - \theta} \right],$$

$$D_2(\theta) = \frac{K}{1+K^2} \left[-\frac{1}{(\theta + 0.5B)^2} + \frac{1}{(0.5A - \theta)^2} \right] + p \frac{1-K^2}{1+K^2} \left[\frac{1}{\theta + 0.5B} + \frac{1}{0.5A - \theta} \right],$$

$$D_4(\theta) = D_0(\theta) \frac{1-K^2}{1+K^2}.$$

The functions $D_1(\theta)$ and $D_5(\theta)$ have the same form as $D_0(\theta)$ and $D_4(\theta)$, respectively, after the replacement $K \to \tilde{K}$ and

$$D_3(\theta) = \frac{\tilde{K}}{1+\tilde{K}^2} \left[-\frac{1}{(\theta + 0.5B)^2} + \frac{1}{(0.5A - \theta)^2} \right] - p \frac{1-\tilde{K}^2}{1+\tilde{K}^2} \left[\frac{1}{\theta + 0.5B} + \frac{1}{0.5A - \theta} \right].$$

Finally, $D_6(\theta, x_0)$ is given by

$$D_6(\theta, x_0) = \frac{1}{\theta} \frac{\sinh(2\theta p)}{\cosh(\theta(x_0 + p)) \cosh(\theta(p - x_0))}. \tag{26}$$

The derived Lagrangian involves four variables x_0, θ, a and b but its equations are rather complicated. Hence, we have solved them numerically. In the next section, we discuss our solutions of the equations which follow from the Lagrangian (25).

4. Results in our effective model

We have looked at the equations for θ, x_0 and a and b, which follow from the Lagrangian (25) and solved them numerically. As our initial conditions we took $x_0 = -40, \theta = 1$ and set, initially, $a = b = 0$. Of course, we also put $\dot{a} = \dot{b} = \dot{\theta} = 0$ and studied the behaviour of our system as a function of $\dot{x}_0$. We also varied a little the parameters A and B, which appear in the description of the effects due to the well. For most of our work we used the values around 0.5 (and used the fact that we expect $A^2 \sim \epsilon + B^2$). To have the well similar to the

one we used in the full simulation (shallow well) we put $\epsilon \sim 0.16$. This is due to the fact that the linearized equations (i.e. for the waves) differ, inside and outside the well, by a term proportional to $\left(\lambda_0^2 - 1\right)u$. In our case, this translates to $A^2 - B^2 \sim \epsilon$ and so for a shallow well we have $\epsilon \sim 1 - \lambda_0^2 = 0.16$.

We simulated the time evolution using the fourth-order Runge–Kutta method and have found that the well distorts the kink quite strongly but, as expected, it can trap the kink like in the original sine-Gordon model. However, as the effective system does not absorb energy after a few bounces the kink can escape (forwards or backwards). Of course, in the real system there are many degrees of freedom of radiation which can get generated in the hole and such bounces are very rare. So to model these 'extra' modes of radiation which take the energy out of the modes we are describing we introduced an absorption of the oscillations of $\theta(t)$, i.e. we added a term proportional to $\dot{\theta}$ in the equation for θ. This has, indeed, reduced the oscillations in θ and made the model more realistic. The obtained curves for $\theta(t)$, see figure 5, where we present them for two cases (trapped and transmitted kinks), were very much as expected. Originally we had $\theta = 1$, then after the kink entered the hole its values changed by about 10–20% (the actual value depended on the strength of the potential) and oscillated over this value while the kink moved in the hole.

As the kink moved into the hole its θ changed. As the kink in an isolated hole is broader initially θ changed down to a smaller value but then due to the interaction with the generated waves started oscillating, in fact, around a value larger than 1. This is seen in figure 5(*a*) for $t \sim 900$. Then, the kink tried to leave the hole. It has almost made it (we present the plots of the case in which the velocity is very close to the critical one). The kink's θ returned to 1 and it remained there as the kink was 'struggling to get out of the hole'. This is seen when one compares $\theta(t)$ with the position(t) seen in figures 5(*a*) and (*c*). Finally, the kink fell back into the hole and oscillated each time when it was coming to the edge of the hole its θ dropping below 1 and then moving above 1. We do not understand this aspect of the motion (except by realizing that this must be due to the interaction with the waves at the edges of the hole). At the same time, the parameters of the excitation of the vacuum, a and b, became nonzero. However, as these excitations were very small a and b were always very small (much less than 1), which justifies our approximation of treating the excitations of the vacuum as a small perturbation.

In figure 6, we present the curve of v_{out} as a function of v_{in} obtained in our model, i.e. based on the Lagrangian (25). We note that although our effective model is quite crude it reproduces figure 3(*b*) rather well. Hence, we believe that the mechanism of Goodman *et al* [10] explains the behaviour of the kinks in our case too. Of course, we could check this in more detail by making fewer approximations and, perhaps, performing the evaluation of all the difficult integrals numerically, but we are not sure that the extra effort required would be justified.

5. Another effective model

Given that our effective model reproduces the results of our simulations rather well we have decided to check the generality of this observation: is this related to the existence of standing waves in the neighbourhood of the well or is our model somewhat unique? Hence, we considered another model this time involving a standing wave in the well. The idea here is to explore further whether the reflections observed in the full model can be related to the interaction of the soliton with the waves in the well. Hence, this time we have taken for our field configuration $\varphi = \varphi_0 + \delta\varphi$, where, as before,

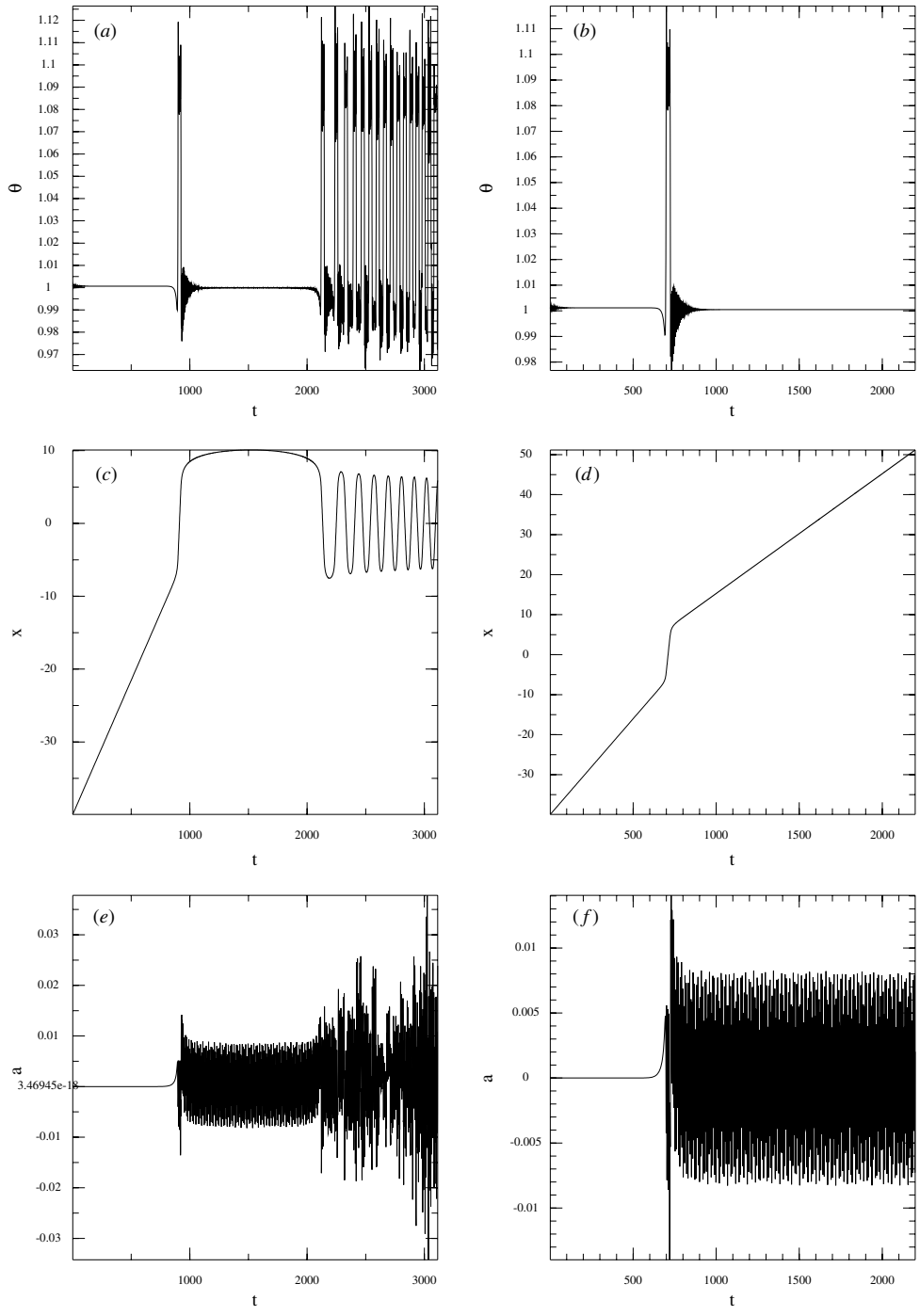

Figure 5. Time dependence of θ (a and b), position (c and d) and parameter a (e and f) for $v = 0.037$ (trapped kink) (a, c and e) and $v = 0.048$ (transmitted kink) (b, d, f).

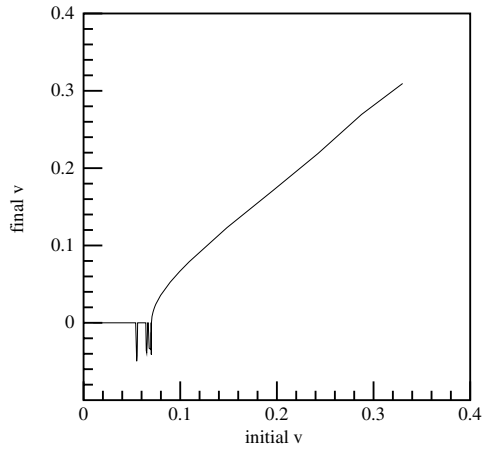

Figure 6. Outgoing velocities as a function of incoming ones—in our effective model.

$$\varphi_0 = 2\tan^{-1}\exp(\theta(t)(x - x_0(t))) \tag{27}$$

and

$$\delta\varphi = a(t)g(x). \tag{28}$$

This time for $g(x)$ we have taken

$$g(x) = \cos\left(\frac{\pi x}{2p}\right) + \frac{1}{3}\cos\left(\frac{3\pi x}{2p}\right) \tag{29}$$

inside the well (i.e. for $|x| < p$ and zero otherwise). Our $g(x)$, and its derivative, vanish at $x = \pm p$ and the idea is that as the soliton enters the well its slope $\theta(t)$ changes. This excites the modes described by $g(x)$ and so $a(t)$ becomes nonzero. This puts some energy into these modes which then interact with the soliton. Due to this interaction this energy can, every now and then, be given back to the soliton resulting in its reflection or transmission.

Our choice for the function $g(x)$ is motivated by the idea that we want to have a standing wave in the hole itself and that we do not want this wave to transmit momentum through the boundaries of the hole (so that $\frac{\partial g}{\partial x}$ vanishes at the boundaries of the hole). We could, of course, have chosen to use the analytical expression for the lowest vibration mode of the well, including the two exponential tails on either side of the well. Unfortunately, this would have resulted in a model that would have been too complicated to study and so we decided to ignore the exponential tails and use (29) to describe the vibrations inside the well.

Like in the previous model, we do not expect such a wave to be an excellent description of what is seen in the full simulations, but we expect it to capture its gross features. Our hope is that this model also reproduces the main features of the simulations of the full model thus supporting our feeling that the origin of the reflections, etc, does lie in the interaction of the kinks with the oscillations of the vacuum set off by the kinks when entering or leaving the region of the hole. If this is confirmed more studies will have to be performed to determine these oscillations and their role in more detail.

Like in the previous model, we have put the expression for φ into the original Lagrangian, integrated over x obtaining an effective model involving x_0, θ and a. Then we performed some simulations starting with a soliton originally far from the well moving with some velocity towards it. Like in the previous model, we have absorbed energy through a term proportional

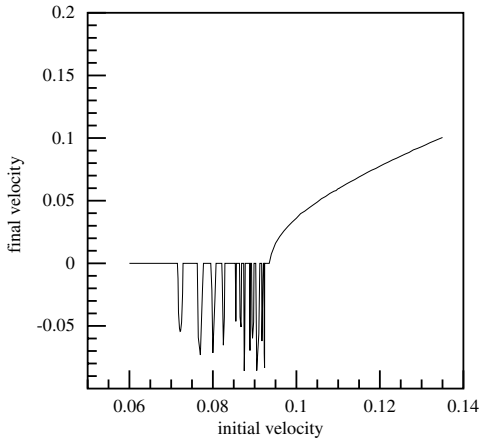

Figure 7. Outgoing velocities as a function of incoming ones—in our second effective model.

to $\frac{\partial\theta}{\partial t}$ in the equation for θ. Also, like in the previous case we have found some reflections below the threshold for the scattering through the well. Their details depend a little on the strength of the absorption: at no absorption we have reflections, and transmissions forward, at much lower velocities, the higher absorptions kill the reflections and transmissions. They also raise the threshold for transmission. Of course, it is difficult to reliably estimate the degree of absorption as in the full model there are many modes of oscillations in the well. So in the end we have used very low absorption; then the threshold for transmission was close enough to what is seen in the full simulation but we had more reflections below threshold. To improve the model, we should have used more modes in the well but this would have resulted in a more complicated model with more degrees of freedom. As we have only wanted to test our basic idea (that the reflections are due to the interaction of the soliton with radiation modes), in this paper, we decided to look at a model which is as simple as possible, i.e., with a very few degrees of freedom. Our choice of two low-lying modes was dictated by simplicity and the basic belief that the lower modes would get excited first and so are more important.

The time dependence of θ was very similar to what was seen in the first effective model, i.e. originally 1, then small perturbation, oscillation around the new value, perturbation and, after further oscillations, gradual return to the original value, i.e., 1. Thus, both models have captured this aspect of the scattering very well. In figure 7, we present the curve of v_{out} as a function of v_{in} obtained in this (second) model (with a reasonable absorption).
Once again, we see that the model reproduces well the pattern of the simulations of the full sine-Gordon model (figure 3(*b*)).

6. Conclusions

We have looked at a system involving a sine-Gordon kink scattering on a 'well'-like potential.

We have found that, like in (2+1) dimensions, when the kink was sent towards the well it gained some energy as it entered the well. Some of this energy was converted into kinetic energy of the kink, some was radiated away. So when the kink tried to 'get out' of the well it had less kinetic energy than at its entry and when this energy was too low it remained trapped in the well. However, as the soliton moved in the 'well' it interacted with the radiation in the well and at some specific values of the initial velocity this interaction resulted in the kink being

ejected backwards from the well (with much reduced velocity). Thus, seen from outside, the well acted as if it reflected the kink, something which is seen in quantum systems but which is less well known in classical systems.

We have performed many numerical simulations to make sure that the observed behaviour is not an unexpected artefact of our numerical procedures and the pattern survived all applied tests. Hence we believe the effect to be genuine.

We have noted that a similar behaviour was observed many years ago by Fei *et al* who studied the scattering of kinks on a one-point impurity. This behaviour was recently explained by Goodman *et al* [10] as a two-bounce resonance between the kink and the oscillation of the defect. This has made us to consider two models of a similar nature. Both models are very simple, clearly too simple, but we wondered whether they would qualitatively reproduce the observed effects. Both involve kinks interacting with radiation and we generate this by taking an ansatz involving a kink (which can vary its position and slope) plus a couple of radiation modes. This ansatz is then put into the full equation which is then integrated out resulting in a model involving a few variables, namely, the position and the slope of the kink and the coefficients of the oscillation modes of the vacuum (modelling radiation).

The first model involved taking standing waves that are located at the edges of the well; the other one involved just one wave in the well. We have found that both models reproduced the main features of the observed behaviour quite well suggesting that the mechanism of Goodman *et al* is more general in nature and that, in general, the observed phenomenon of reflection of the solitons on the well is related to their interaction with the waves in the well. Of course, both models are too simplistic; to describe properly the full process we have to understand better which modes of radiation are important and why. This involves more work and is planned for the future. However, the work done so far suggests that we are on the right track and gives us encouragement for the further study. This is confirmed further by what we saw in a two-dimensional model [2] in which the solitons have genuine vibrational as well as radiation modes.

Incidentally, in our calculation we have used the correct initial condition, i.e., with the correct relativistic factors $\left(\gamma = \frac{1}{\sqrt{1-v^2}}\right)$. Of course, missing such factors would not make sense, but on the other hand this factor is very very close to 1 for small velocities and so at first sight may appear not to be very important. To check this we have decided to study the effects of its absence—which in large part is equivalent to picking a slightly 'wrong' initial slope θ. Thus, had we ignored γ factors and used the nonrelativistic form of the initial condition (i.e. not modified θ in (10) and (26)) we would have obtained instead of figure 7 the dependence which is shown in figure 8. We note an interesting oscillatory behaviour. This oscillation resembles very closely the oscillation of $\theta(t)$ seen in both effective models. Of course, when the kink enters a hole it does have a 'wrong' θ so it changes it to a more appropriate value, overshooting a bit, and this leads to an oscillation in θ. Here we did start with 'wrong' θ and not surprisingly this leads to the oscillations from the start and overall much larger oscillations. Of course, the oscillation in our case is overemphasized by the use of too few radiation modes but we wondered whether it would be seen in the full model too (i.e. whether the addition of further modes would wash them out). Hence, we also have redone the full simulations without the relativistic factors. Our nonrelativistic curve is shown in figure 9. We note the extra oscillations. Their origin lies clearly in the fact that the absence of γ factors induces initial distortions resulting in the change of θ. This affects the phase of the soliton and so alters its interaction with the wave in the well resulting in the curve shown in figure 9. It is interesting to note that our effective models also reproduce these oscillations, thus giving further support for the validity of our claim that the interaction with the well proceeds through the generation of standing waves and their interference with the solitonic fields. Of course,

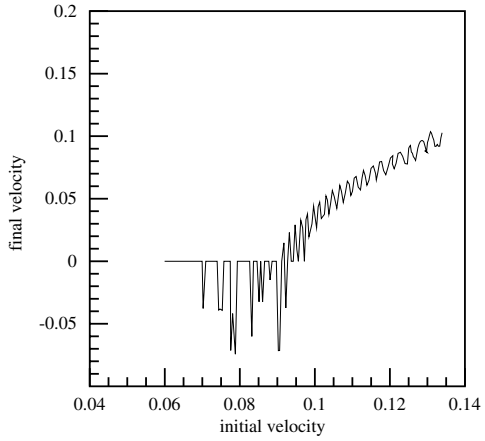

Figure 8. Outgoing velocities as a function of incoming ones—in our second effective model without relativistic corrections.

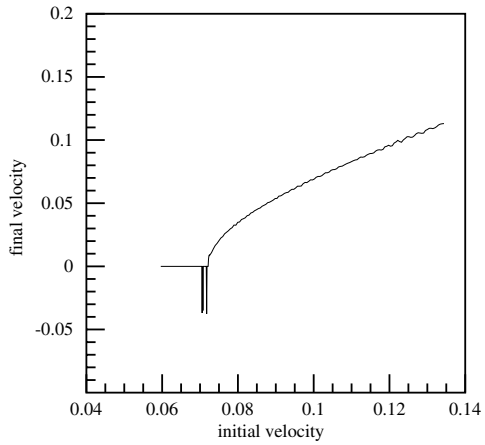

Figure 9. Outgoing velocities as a function of incoming ones—in the full simulation without relativistic corrections.

the agreement between the results of the full simulations and of the effective models is only qualitative in nature as in our effective models we used only some standing waves which were chosen somewhat ad hoc. To get a quantitative agreement we have to determine the relative importance of different waves—this problem is currently under consideration.

As briefly mentioned in the introduction, a wide class of physical systems are described by the sine-Gordon equation, especially in solid state physics, and it would be interesting to see what the physical implications of a position-dependent potential, like the one used in this paper, would be.

Let us finish by adding that there have been many other studies of the sine-Gordon model (for a good review see, e.g., [18]). Some of them involved adding 'boundaries' or sewing up solutions of sine-Gordon models with different parameters while still preserving their integrability [19, 20]. In those papers there were regions of spatial variable x in which λ was

different; and then at the junction points the boundary conditions were imposed so that such models were integrable. The requirement of integrability (see [20]) involved derivative terms, etc, on the boundary. In our case, we require the continuity of the function and its derivative; hence our model is non-integrable and so the change of the potential leads to the effects that we have discussed.

Acknowledgments

This investigation is a natural follow-up of the work on (2+1)-dimensional topological solitons originally performed in collaboration with Joachim Brand. We would like to thank him for this collaboration. We would like to thank R H Goodman for drawing our attention to the long review of B A Malomed [11].

References

[1] Piette B M A G, Zakrzewski W J and Brand J 2005 *J. Phys.: Condens. Matter* **A** 1–10
[2] Piette B M A G and Zakrzewski W J 2007 *J. Phys. A: Math. Theor.* **40** 329–46
[3] Fei Z, Kivshar Yu S and Vazquez L 1992 *Phys. Rev.* A **45** 6019–30
[4] Peyrard M and Campbell D K 1983 *Physica* D **9** 33–51
[5] Campbell D K and Peyrard M 1983 *Physica* D **18** 47–53
[6] Campbell D K, Schonfeld J S and Wingate C A 1983 *Physica* D **9** 1–32
[7] Scott A 1999 *Nonlinear Science* (*Oxford Applied and Engineering Mathematics* vol 1) (Oxford: Oxford University Press)
[8] Goodman R H, Slusher R E and Weinstein M I 2002 *J. Opt. Soc. Am.* B **19** 1635
[9] Goodman R H, Holmes P J and Weinstein M I 2002 *Phys. Rev.* D **161** 21–44
[10] Goodman R H and Haberman R 2004 *Physica* D **195** 303–23
[11] Malomed B A 2002 *Prog. Opt.* **42** 71–193
[12] Josephson B D 1974 *Rev. Mod. Phys.* **46** 251–4
[13] Perring J K and Skyrme T H R 1962 *Nucl. Phys.* **31** 550–5
[14] Abdalla E, Maroufia B, Melgara B C and Sedrab M B 2001 *Phys. A: Stat. Mech. Appl.* **301** 169–73
[15] McCall S and Hahn E L 1969 *Phys. Rev.* **183** 457
[16] Wysin G, Bishop A R and Kumar P 1984 *J. Phys. C.: Solid State Phys.* **17** 5975–91
[17] Speight J M and Ward R S 1994 *Nonlinearity* **7** 475–84
[18] Ablowitz M J and Clarkson P A 1991 *Solitons, Nonlinear Evolution Equations and Inverse Scattering* (Cambridge: Cambridge University Press)
[19] Corrigan E 2006 Purely transmitting integrable defects *Preprint* hep-th/0609134
[20] Bowcock P, Corrigan E and Zambon C 2004 *Int. J. Mod. Phys.* A **19** 82 (*Preprint* hep-th/0305022)